Quantitative Determination of Helical Propensities from Trifluoroethanol Titration Curves†

Alan Jasanoff‡ and Alan R. Fersht*

MRC Unit for Protein Function and Design, Department of Chemistry, Lensfield Road, Cambridge CB2 1EW, U.K.

Received October 15, 1993; Revised Manuscript Received December 9, 1993®

ABSTRACT: The formation of local secondary structure is an essential step in the folding of a polypeptide from a random coil to a well-defined native conformation. Detection of hidden structural propensities in amino acid sequences may provide important insight into how this is accomplished. 2,2,2-Trifluoroethanol (TFE) has been shown to induce helical structure in polypeptides, and TFE titration has been used as a qualitative probe for helical tendency. We have investigated the propensity of five synthetic peptides to adopt helical structure in TFE. The free energy of helix formation exhibits linear dependence on the mole ratio of TFE to water, and the constant of proportionality (m-value) can be perturbed systematically by altering the peptide length and unsystematically by altering the temperature. Three peptides with closely related sequences but different N-cap residues show different titration behavior from 5 to 75 °C, suggesting that TFE acts only within the context of a preexisting helix–coil equilibrium. These observations can be reconciled with a model for TFE/H_2O exchange at peptide binding sites. Our results support the viability of TFE titration as a tool for extrapolation of quantitative helix–coil equilibrium constants for peptides with little or no apparent helical content in aqueous solution.

The existence of compounds that stabilize secondary structure in peptides and proteins has long been known (Doty et al., 1954). Like denaturants, which have been used to study the free energy change on protein unfolding, these structure-inducing compounds provide useful probes of the tendency of polypeptides to adopt structure in solution. High concentrations of sodium dodecyl sulfate and several weakly polar alcohols such as methanol, 2,2-dichloroethanol, and in particular 2,2,2-trifluoroethanol (TFE) have been used to induce helical structure in peptides (Doty et al., 1954; Conio et al., 1970; Liebes et al., 1975; Nelson & Kallenbach, 1986). CD and NMR experiments have shown that the characteristic spectroscopic features of α-helices in proteins are present also in the spectra of TFE-induced helices (Dyson et al., 1988; Bruch & Hoyt, 1992; Storrs et al., 1992; Sonnichsen et al., 1992; Shin et al., 1993). The precise mechanism of structure induction by TFE is unknown. It has been observed in the context of denaturant binding studies that a solvent component that interacts preferentially with one of a peptide's microscopic states tends to shift the conformational equilibrium toward that state (Schellman, 1990; Creighton, 1991), so it may be reasonable to expect that TFE acts by selective association with the helical conformation of a peptide.

Previous experiments have shown that the CD spectra of randomly coiled or partially structured polypeptides, including some polypeptides in β-sheet conformation, generally exhibit a sharp transition as TFE concentration is increased above a critical value (Liebes et al., 1975; Fan et al., 1993). In particular, the optical rotation at 222 nm, which is generally assumed to be proportional to helical content, exhibits sigmoidal dependence on TFE concentration, indicating that the induction of helical structure by TFE is a cooperative process (Liebes et al., 1975; Sancho et al., 1992). This can be reconciled with the theoretical models of helix formation proposed by Zimm and Bragg (1959) and Lifson and Roig (1961) by assuming that TFE increases the statistical weight of each residue in helical conformation (s), rather than affecting helix initiation through the nucleation parameter (σ). TFE structure induction has also been analyzed in terms of a two-state model for the helix formation. Titration data were found to be consistent with a linear dependence on TFE concentration of the free energy of helix–coil interchange (Sancho et al., 1992).

Table 1: Peptide Sequences

peptide	sequence[a]
D12	**D** P A **E** A A **K** A A A G R
N12	**N** P A **E** A A **K** A A A G R
E12	**E** P A **E** A A **K** A A A G R
D10	**D** P A **E** A A **K** A G R
D14	**D** P A **E** A A **K** A A A A A G R

[a] All peptides are C-terminally amidated, but not N-terminally carboxylated. Residues in bold are involved in sequence variations.

In the present study of helix induction by TFE, we have used three peptides used in a previous study on the effects of capping residues on α-helicity (Forood et al., 1993) and two peptides related to those. Their sequences are given in Table 1. Peptides D12, N12, and E12 (12 residues) are used in order to relate the inherent helical tendencies of the peptides to the ability of TFE to induce further helical structure at different temperatures. Peptides D10, D12, and D14 (10, 12, and 14 residues) are designed to test the effect of chain length on TFE induction. We have examined the effect of temperature and chain length on the circular dichroism (CD) spectra of the peptides at various concentrations of TFE. Short peptides have been used in order to minimize the possibility of nonhelical structure formation. Our results are consistent with accepted theoretical models for helix formation and solvent–solute interactions and suggest that TFE titration may

† A.J. was supported by a Herchel Smith Scholarship.

* To whom correspondence should be adressed.

‡ Present address: Howard Hughes Predoctoral Fellow, Committee on Higher Degrees in Biophysics, Harvard University, Cambridge MA 02138.

® Abstract published in *Advance ACS Abstracts,* February 1, 1994.

0006-2960/94/0433-2129$04.50/0

reasonablybe used as a quantitative probe for helical tendency in polypeptides.

METHODS AND MATERIALS

Peptide Synthesis and Purification. Peptides were synthesized on a Synergy Personal Peptide Synthesizer (Applied Biosystems) which performs solid-phase synthesis using 9-fluorenylmethylcarbonyl (F-moc) protection and 2-(1*H*-benzotriazol-1-yl)-1,1,3,3-tetramethyluronium hexafluorophosphate (HBTU) activation chemistry. Cleavage from the resin was performed with a TFA/thioanisol/ethanediol mixture. The peptides were purified and assayed by absorbance at 215 nm using a Gilson high-pressure liquid chromatography (HPLC) apparatus with Rainin-Dynamax reversed-phase analytical and preparative columns and a gradient of 5–30% acetonitrile (0.1% TFA). Purified peptides were lyophilized and stored at −70 °C.

CD Measurements and Analysis. For all experiments, the peptides were dissolved in 0–90% TFE (volume of TFE added/total volume added) and 5 mM potassium phosphate, pH 7.4 ($[KH_2PO_4]/[K_2HPO_4]$ = 0.511). Titrations and thermal scans were performed in a 1-mm-path-length cell with peptide concentrations between 10 and 100 μM, at which the 12 residue peptides have been shown to be monomeric in solution (Forood et al., 1993). Concentration independence of the CD signal was also established for peptides D10 and D14. CD measurements were made on a Jasco 720 spectropolarimeter with a Neslab temperature controller. Wavelength scans were performed at 25 °C from 180 to 260 nm, and thermal scans were performed at 222 nm from 5 to 75 °C. Baselines were subtracted from the CD data. Peptide compositions were verified and sample concentrations were determined by amino acid analysis.

Data Analysis. Data were analyzed using the Kaleidagraph package (Abelbeck Software). Thermal data were smoothed by least-squares weighted fitting to Stineman functions. Titration data were analyzed by unweighted least-squares fitting to theoretical titration curves, assuming (unless otherwise stated) direct proportionality between mean residue ellipticity at 222 nm ($[\Theta]_{222}$) and helical content.

Model for TFE–Peptide Interactions. Two functions were used in curve fitting to account for the free energy effect of TFE on the peptide equilibrium, assuming a two-state model for the helix–coil transition. The first model assumes that the free energy of helix formation is linear with the percent of TFE in the solution and has been shown to fit the data from a TFE titration of helices in barnase (Sancho et al., 1992). This relationship has been used to describe the effects of urea and guanidinium chloride as protein denaturants [review articles: Tanford (1968) and Pace (1986)] and can be expressed in the following equation:

$$\Delta G^{[TFE]} = \Delta G^{H_2O} - m[TFE] \quad (1)$$

where ΔG^{H_2O} is the free energy of helix formation in water, $\Delta G^{[TFE]}$ is the free energy of helix formation in a given concentration of TFE, and m is the m-value.

The m-value relationship can be derived from a simple weak-binding model for TFE–peptide interaction,

$$\text{coil}\cdot(n'\text{TFE}) \overset{K_{bind}^{coil}}{\rightleftharpoons} n'\text{TFE} + \text{coil} \overset{K_{helix\ formation}}{\rightleftharpoons} n\text{TFE} + \text{helix} \overset{K_{bind}^{helix}}{\rightleftharpoons} \text{helix}\cdot(n\text{TFE})$$

in which the binding of TFE contributes polynomial factors to the numerator and denominator of the equilibrium constant for helix formation:

$$K_{\text{helix formation}}^{[TFE]} = K_{\text{helix formation}}^{H_2O}\cdot\left\{\frac{(1 + K_{bind}^{helix}\cdot[TFE])^n}{(1 + K_{bind}^{coil}\cdot[TFE])^{n'}}\right\} \quad (2)$$

where K_{bind}^{helix} and K_{bind}^{coil} are the binding constants for TFE to the helix and coil states of a peptide with n and n' non-interacting binding sites in helix and coil, respectively. Using the well-known mathematical result that $\lim_{n\to\infty}(1 + x/n)^n = e^x$, the above expression simplifies, for large enough n and n', to:

$$K_{\text{helix formation}}^{[TFE]} = \delta K_{\text{helix formation}}^{H_2O}\exp\{(nK_{bind}^{helix} - n'K_{bind}^{coil})[TFE]\} \quad (3)$$

This equation reduces to the form of eq 1 on taking the logarithm of each side and multiplying by R, the gas constant, and T, the temperature. The m-value is:

$$m = RT(nK_{bind}^{helix} - n'K_{bind}^{coil}) \quad (4)$$

where n and n' are the number of TFE binding sites in helix and coil states. If the number of interacting sites in the helix and coil differ, the influence of a ligand such as TFE could be predominantly due to binding to a different number of sites in helical and coiled peptides ($\Delta n = n - n'$). Since both n and K_{bind} are average properties reflecting probabilistic binding to different but similar sites, and because the helix–coil transition does not involve variable change in the solvent exposure of similar participating functional groups (as occurs with the burial of side chains in protein folding), we have chosen to approximate the system with n sites in both helix and coil states. This simplifies analysis of the m-value, which can now be expressed as a product of n and K_{bind}, $nRT(K_{bind}^{helix} - K_{bind}^{coil})$, where n is the number of interacting sites in both helix and coil. Under this approximation, $K_{bind}^{helix} > K_{bind}^{coil}$ is a condition sufficient for stabilization of helical structure by TFE.

Since binding of TFE to a peptide likely involves displacement of bound water molecules from the binding sites, the peptide–TFE interaction is more accurately modeled as an exchange between water and TFE:

$$\text{peptide}\cdot(n\text{TFE}) + n\text{H}_2\text{O} \overset{K_{exch}^{helix}}{\rightleftharpoons} \text{peptide}\cdot(n\text{H}_2\text{O}) + n\text{TFE}$$

A detailed analysis of protein–solute interactions as selective interactions has been presented previously by Schellman (1990). Consideration of binding exchange is more important in modeling the effects of TFE than in modeling the effects of urea, because the relative activity of water in solution drops far more over typical experimental ranges of [TFE] than it does over typical ranges of [urea].

Assuming that each binding site is always occupied either by water or by TFE, the expression for the helix–coil equilibrium constant becomes

$$K_{\text{helix formation}}^{[TFE]} = K_{\text{helix formation}}^{H_2O}\left\{\frac{(1 + K_{exch}^{helix}[TFE]/[H_2O])^n}{(1 + K_{exch}^{coil}[TFE]/[H_2O])^{n'}}\right\} \quad (5)$$

where K_{exch}^{helix} and K_{exch}^{coil} are the equilibrium constants for

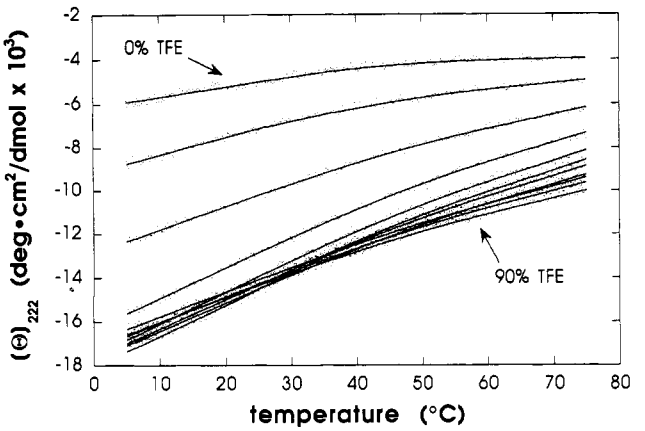

FIGURE 1: Thermal scans ($[\Theta]_{222}$ vs temperature) for peptide N12 in 11 concentrations of TFE ranging from 0–90% (thin arrows) by intervals of 9%. Smooth curves have been fitted to the data.

TFE–water exchange in the helix and coil states. In this case, the following free energy relationship is derived:

$$\Delta G^{[TFE]} = \Delta G^{H_2O} - m[TFE]/[H_2O] \quad (6)$$

where m is now $RT(nK_{exch}^{helix} - n'K_{exch}^{coil})$ and $[TFE]/[H_2O]$ is the mole ratio of the two components in solution. We will simplify m as previously, by assuming an equal number of binding sites in helix and coil states, and express the difference in binding/exchange constants to helix and coil states as $K_{bind/exch}$. This gives m as

$$m = nRTK_{bind/exch} \quad (7)$$

Both this approximation and the TFE binding approximation are more valid for peptides with many binding sites. The two models are equivalent at low [TFE].

RESULTS

Temperature Dependence of TFE Helix Induction. Thermal melting curves for peptide N12 in 0–90% TFE, monitored by CD at 222 nm, are shown in Figure 1. Similar results were obtained for peptides D12 and E12. The curves are almost linear with temperature, indicating that ΔH associated with the global helix–coil transition is small or that the melting is uncooperative, as indicated by previous calorimetric studies (Scholtz et al., 1991a). In the case of peptide E12 at low percent TFE, an increase in CD amplitude at 222 nm is seen with increasing temperature (data not shown). Such an increase has been seen previously for this and other peptides supposed to be in random coil conformation (Forood et al., 1993; Scholtz et al., 1991b; Doty & Yang, 1956) and could reflect intrinsic dependence of CD on temperature, the presence of nonhelical residual structure in the coil state with ellipticity at 222 nm, or an increase with temperature of the equilibrium constant for helix formation (positive ΔH). The thermal data have been transformed into titration curves at specific temperatures (5–75 °C) to facilitate further analysis (Figure 2). Curve fitting to the data is complicated by the absence of linear baselines at low percent TFE. The decreasing amplitude of the overall change in $[\Theta]_{222}$ with temperature may be due to a number of factors including melting of the titrated helices, decrease in the amplitude of $[\Theta]_{222}$ for helical residues at higher temperature, and thermally induced solvent expansion. For all three peptides $[\Theta]_{222}$ at 25 °C approaches −15 000 deg cm² dmol⁻¹, which corresponds to roughly 50% helicity assuming a value of −31 500 deg cm² dmol⁻¹ for 100%

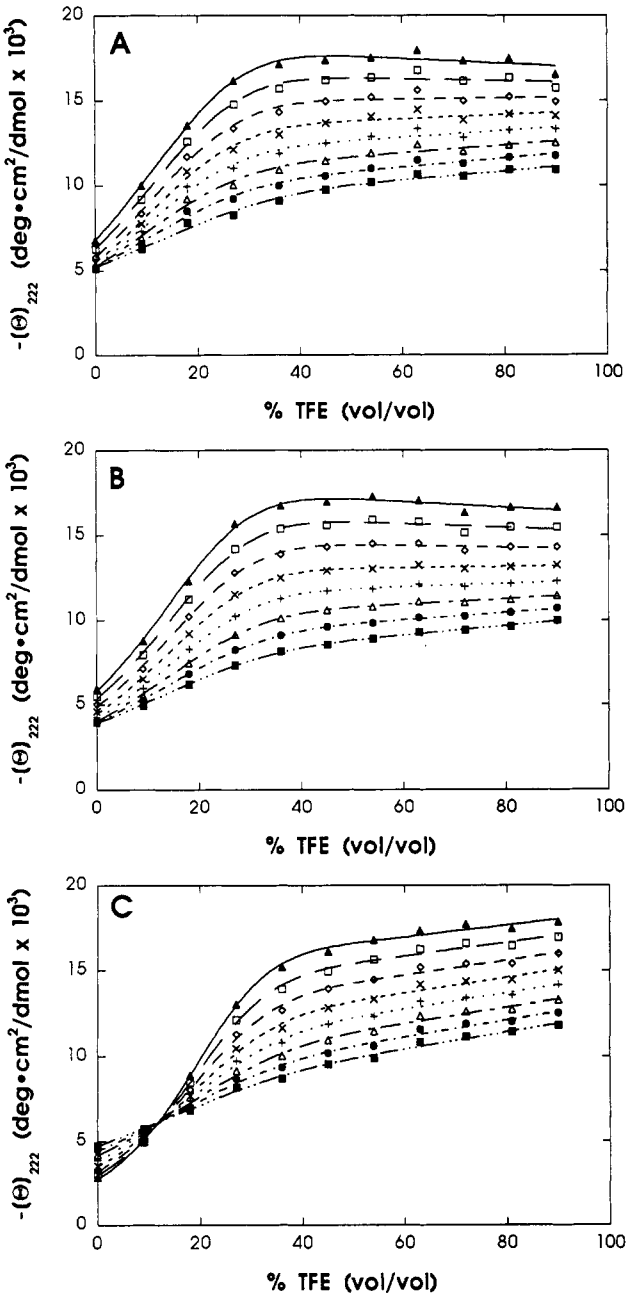

FIGURE 2: TFE titrations transformed from thermal scans for three peptides, (A) D12, (B) N12, and (C) E12. Fitted curves are derived from the TFE/H_2O exchange model (eq 6). Temperatures increase in order of decreasing $[\Theta]_{222}$ amplitude from 5 °C (▲) to 75 °C (■), by intervals of 10°.

helicity of a 12-residue peptide (Forood et al., 1993). This suggests that the ability of different N-cap residues to stabilize helical structure by varying degrees is immaterial in high [TFE] for short peptides.

Fitting of the data to equations for TFE binding (eq 1) and TFE/H_2O exchange (eq 6) yields values for $K_{helix\ formation}$ and m. Plots of $K_{helix\ formation}$ and m, assuming direct proportionality of helicity to $[\Theta]_{222}$, against temperature are shown in Figure 3. The plots indicate a smooth increase in K with temperature for all three peptides. Values for K are dependent on the choice of the random coil $[\Theta]_{222}$ baseline value, but the increasing trend in K is observed when data is fit to either TFE interaction model (eq 1 or 6). Values for K as determined by the two models at 5 and 25 °C are summarized in Table 2. Somewhat different K values are obtained using the two models. Although there is good correlation between measured

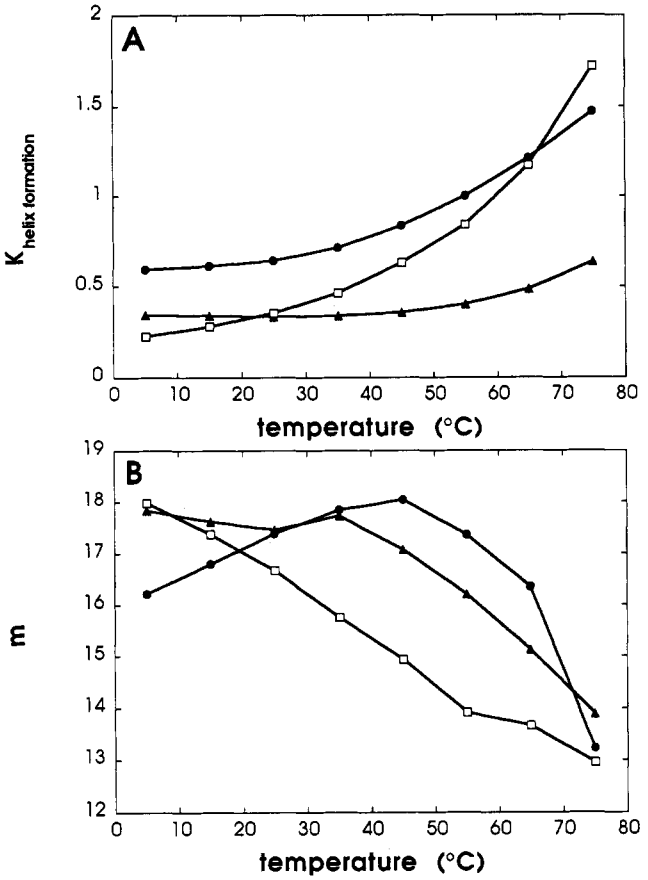

FIGURE 3: Development of (A) $K_{helix\ formation}$ and (B) m with temperature for peptides D12 (●), N12 (▲), and E12 (□). Values are obtained from fits to the TFE/H_2O exchange equation (eq 6).

$[\Theta]_{222}$ values and $K_{helix\ formation}$ at either temperature, fractional helicities calculated from helix equilibrium constants from the expression $K_{helix\ formation}/(1 + K_{helix\ formation})$ consistently exceed fractional helicities calculated from absolute ellipticity values (Forood et al., 1993). There need be no inconsistency between the two sets of results, because Farood et al. measured simply the fraction of the residues that are present as helix, whereas we have measured the equilibrium constant between helix and coil in $K_{helix\ formation}$. The two methods should give the same fractional helicity only when all 12 residues of each peptide are helical. The discrepancy indicates that not all of each peptide is helical. It should be noted in this context that the nature of the equilibrium between helical and nonhelical peptide conformations could be dependent on temperature, so an equilibrium constant at 5 °C could well correspond to a different transition from that for the equilibrium at 75 °C. This is also indicated by the absence of an isodichroic point in the peptides' CD spectra as the temperature is raised (Forood et al., 1993). An increase in K with temperature for any given transition could reflect either the influence of ΔC_p or a positive ΔH for helix formation, given that

$$\ln K_{helix\ formation} = -\frac{\Delta H^\circ + \Delta C_p(T - T_m)}{RT} + \frac{\Delta S^\circ + \Delta C_p \ln (T/T_m)}{R} \quad (8)$$

where T_m is the midpoint temperature for the transition and ΔH° and ΔS° are the enthalpy and entropy changes at T_m, assuming reasonably that ΔC_p is constant with temperature (Privalov, 1979). In proteins, ΔC_p is generally proportional to the degree of side-chain burial upon folding, which is small in the case of helix formation in a peptide, suggesting that the increase in $K_{helix\ formation}$ is more likely due to positive enthalpy. Small values of ΔC_p for helix formation have been predicted by Ooi and Oobatake (1991). Positive enthalpy for per-residue helix formation was predicted by both the Zimm and Bragg (1959) and the Lifson and Roig (1961) models and may be due to removal of solvent from the peptide surface as the helix is formed.

The dependence of the m-value for TFE structure induction on temperature is less straightforward (Figure 3). Trends in m with temperature, like K, are dependent on the choice of initial baselines. Regardless of the choice of baselines, however, peptides D12 and N12 show fairly similar development of m with temperature, while E12 exhibits a different pattern. According to both the TFE binding and the TFE exchange model, m is the product of an equilibrium constant for binding/exchange with the number of sites for TFE–peptide interaction (n). $K_{bind/exch}$ and its temperature dependence should be roughly the same for all peptides, since it is a general property of TFE association with individual binding sites. Values for n, and its variation with temperature, could be significantly different depending on the sequence of the peptide and the corresponding helix–coil equilibrium in solution.

The study of Forood et al. (1993) indicated that the N-cap interactions of the D12 and N12 peptides are at least partially formed at 5 °C and that D12 and N12 are more fully helical than E12, which has a poor N-cap residue (Glu). Differences between the m-values of these peptides possibly reflect differences in the degree of formation of the N-cap interactions throughout most of the temperature range. The m-values of all three peptides appear to approach the same value at higher temperatures, possibly indicating melting of N-cap interactions. $[\Theta]_{222}$ for these and related peptides in water also approaches a common limiting value at high temperature (Forood et al., 1993). Final (high [TFE]) baselines for the three peptides also approach a common slope at high temperature. The slopes of these baselines vary with temperature and peptide sequence and may reflect chiral organization of (achiral) solvent molecules around the helical peptides.

Dependence of TFE Helix Induction on Peptide Length. The titration curves obtained for peptides D10, D12, and D14 are shown in Figure 4A. Observation of an isodichroic point near 203 nm in the CD spectra of the peptides as [TFE] is increased (Figure 5) supports the assumption that at any given temperature the helix–coil interchange can be considered a two-state process (Holtzer & Holtzer, 1992). Assuming direct proportionality of helicity at 25 °C to $[\Theta]_{222}$, data from all three peptides fit better to the TFE/H_2O exchange model than to a TFE binding model. The TFE binding model can be accommodated by assuming a baseline random coil $[\Theta]_{222}$ value near −3000 deg cm^2 dmol^{-1}, which is significantly below predicted and observed values for random coil $[\Theta]_{222}$ under similar conditions. Transformation of titration data to plots of ln $K_{helix\ formation}$ vs percent TFE illustrates curvature that can be explained by the exchange model but not by the binding model (Figure 4B).

When fit to the TFE exchange model, the 10-, 12-, and 14-residue peptides give values for $K_{helix\ formation}$ of 0.53 ± 0.02, 0.59 ± 0.02, and 0.80 ± 0.03; values for m (kcal mol^{-1}) are 14.6 ± 0.6, 16.6 ± 0.5, and 21.3 ± 1.1. When fit to the TFE binding model, values are 0.39 ± 0.02, 0.49 ± 0.02, and 0.72 ± 0.03 for K and 0.077 ± 0.004, 0.085 ± 0.003, and 0.104 ± 0.007 for m [kcal mol^{-1} (% TFE)$^{-1}$]. In these titrations, and in other TFE titration curves obtained from peptides constructed with barnase and chymotrypsin inhibitor

Table 2: Equilibrium Constants for Helix Formation[a]

peptide	% helicity	5 °C $[\Theta]_{222}$	5 °C K^{TFE}	5 °C K^{TFE/H_2O}	25 °C $[\Theta]_{222}$	25 °C K^{TFE}	25 °C K^{TFE/H_2O}
D12	25.1	6800	0.50 ± 0.03	0.59 ± 0.04	5800	0.54 ± 0.04	0.64 ± 0.05
N12	24.4	5921	0.40 ± 0.04	0.34 ± 0.02	5000	0.41 ± 0.03	0.33 ± 0.02
E12	8.6	2800	0.18 ± 0.01	0.23 ± 0.02	3240	0.28 ± 0.02	0.35 ± 0.03

[a] Percent helicity values proportional to mean residue ellipticity of peptides in 10 mM KF at 0 °C, pH 7, are obtained from Forood et al. (1993). K^{TFE} and K^{TFE/H_2O} are equilibrium constants for helix formation in water, $K_{\text{helix formation}}^{H_2O}$ in eqs 3 and 5, calculated from titration curves using the TFE binding equation (eq 1) and the TFE/H_2O exchange equation (eq 6), respectively. These values and $[\Theta]_{222}$ measurements were recorded in 5 mM potassium phosphate, pH 7.4.

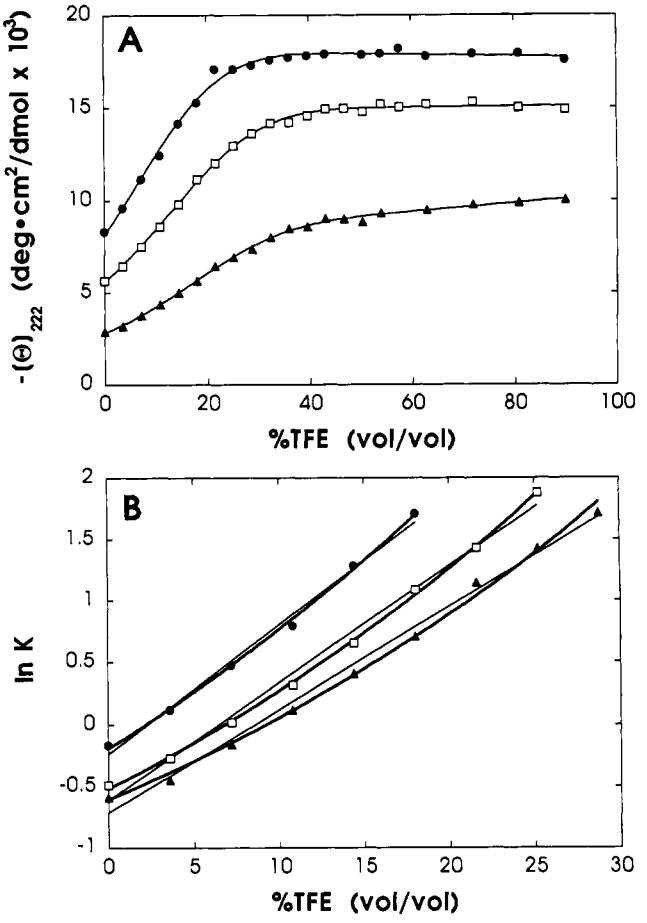

FIGURE 4: (A) Titration curves for three peptides of different length, D10 (▲), D12 (□), and D14 (●). Fitted curves are derived from the TFE/H_2O exchange equation (eq 6). (B) Comparison of fittings based on the TFE binding equation (thin lines) and the TFE exchange equation (heavy lines). The titration data from panel A have been transformed to give a plot of ln K vs percent TFE in the titration transition region.

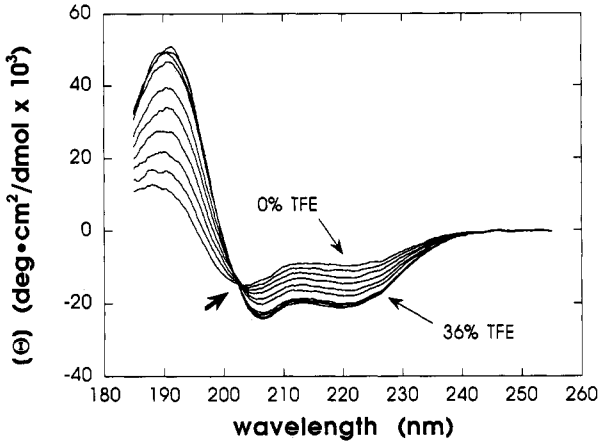

FIGURE 5: CD spectra of peptide D14 at different [TFE] ranging from 0–36% (thin arrows) by intervals of 3.6%. There is an isodichroic point at 203 nm (thick arrow).

2 helix sequences (A. Kippen and J. Ruiz-Sanz, unpublished data), the simple binding model underestimates K with respect to the exchange model. The difference is more acute for peptides that titrate at higher percent TFE, where the models diverge further from one another due to increasing [TFE]/[H_2O].

The increase in $K_{\text{helix formation}}$ with peptide length could reflect the increasing population of alanine residues, which have higher than average helical propensities as indicated by a variety of approaches (Sueki et al., 1984; Richardson & Richardson, 1988; Chakrabartty et al., 1990; Lyu et al., 1990; O'Neil & DeGrado, 1990; Wojcik et al., 1990; Horovitz et al., 1992). According to the Zimm and Bragg (1959) and Lifson and Roig (1961) models, the rate-determining step in helix formation is a single residue-dependent nucleation step, while helix denaturation depends on the loss of helical structure in all contributing residues. This would also lead to an increase in $K_{\text{helix formation}}$ with peptide length. An increase in percent helical content with chain length has been observed previously in peptides with repetitive sequences of different length (Scholtz et al., 1991b).

The m-values for TFE induction are proportional to the number of residues in the peptides, as predicted by both theoretical models for TFE helix induction. A linear fit to the three data points in a plot of peptide length vs m-value extrapolates to a y-intercept close to zero, which suggests that proportionally many residues in each length peptide are involved in interactions with TFE at this temperature (25 °C). Proportional dependence of the m-value on chain length is virtually independent of the choice of random coil $[\Theta]_{222}$ baseline for variation of TFE.

DISCUSSION

The temperature and peptide-length dependence of the TFE titration curves of five synthetic peptides have been studied using CD at 222 nm. Equations based on two simple models for the TFE–peptide interaction have been used to fit the data, and they give close agreement with experimental results. Both models predict linear dependence of the slope of the free energy of helix formation (m-value) on the length of the peptide, which we have observed in peptides D10, D12, and D14. Because increases in the length of these peptides involve only the addition of alanine residues (Table 1), it is unlikely that the effect of TFE as manifested in the m-value involves side-chain electrostatics. If $[\Theta]_{222}$ at 25 °C is assumed to be directly proportional to helicity, a model based on an assumption that TFE binding is accompanied by dissociation of water from individual sites on the peptide (TFE/H_2O exchange, eq 6) gives a closer fit to the data than a simple TFE binding model (eq 1), and the two give somewhat different values for $K_{\text{helix formation}}$. Exchange models are necessary in

the description of systems where the activity of one influential solvent component (in this case water) decreases significantly as the activity of another (TFE) is increased. If the TFE/H_2O exchange model is physically accurate, it may account for the relatively low range of midpoints (<30%, vol/vol) generally observed in TFE titrations of helical structure in peptides, since the relative activity of TFE in TFE/H_2O solutions increases much more rapidly as [TFE] increases and binding sites could become saturated at relatively low percent TFE.

Studies of the development of TFE titration curves with temperature for three peptides, D12, N12, and E12, indicate that the titration *m*-value and $K_{\text{helix formation}}$ can differ significantly between closely related peptide sequences and that the two observables vary significantly with temperature. The absence of linear $[\Theta]_{222}$ baselines at low percent TFE for these titrations renders difficult absolute measurements of the quantities without additional assumptions concerning the CD spectra of random coil peptides. According to the interaction models presented here, temperature development of the *m*-value may be due to changes in the equilibrium constants for TFE binding or exchange with water ($K_{\text{bind/exch}}$) and to changes in the number of residues involved in the putative two-state helix–coil equilibrium (*n*).

Differences in the temperature development of the *m*-values for D12, N12, and E12 titrations are more likely to reflect differences in the development of *n* with temperature, because $K_{\text{bind/exch}}$ is an average physical parameter based on association of TFE and water with individual sites on the peptide. The number of sites accessible to interaction with TFE is presumably dependent on local breathing in the peptide and on retention times for bound solvent molecules and could be expected to be temperature dependent. This would be consistent with the observation of $\Delta H_{\text{cal}} >> \Delta H_{\text{vH}}$ in calorimetric studies of a 50-residue peptide, which indicates that melting of helical structure is a multistate process (Scholtz et al., 1991a). Further, the fact that the *m*-value varies significantly with relatively conservative changes in peptide sequence (Asp to Glu) suggests that TFE acts within the framework of an existing helix–coil equilibrium, a hypothesis also supported by studies on the S-peptide of ribonuclease A (Nelson & Kallenbach, 1989; Storrs et al., 1992).

It has been suggested in previous investigations that the induction of helices by TFE is a thermodynamic, or medium, effect, which is independent of specific interactions between TFE and the polypeptide chain and is manifested in weakened hydrogen bonding between solvent and the peptide coil state (Conio et al., 1970; Storrs et al., 1992). A number of experimental results do not fully support this hypothesis, notably the fact that TFE does not appear to stabilize secondary structure in general and the ability of TFE to induce helical structure in sequences already in or with a preference for β-sheet conformation (Zhong & Johnson, 1992; Fan et al., 1993). The failure of TFE to alter the pH dependence of the stability of the ribonuclease A S-peptide helix has been used as evidence that helix induction by TFE is not due to its dielectric properties (Nelson & Kallenbach, 1986), but the possibility that macroscopic or colligative properties of mixed TFE/H_2O solutions play a role in TFE helix induction, in addition to proposed binding or exchange effects, cannot be rejected on the basis of existing data.

Wemmer and co-workers argue that the failure of TFE to influence the nuclear Overhauser effect (NOESY) spectrum of a disulfide-engineered analogue of the S-peptide is evidence against explicit TFE–peptide interactions (Storrs et al., 1992). Manifestation of specific solvent–solute interactions in enhanced spin diffusion rates, relaxation rates, or detectable solvent–solute rotating-frame Overhauser enhancements (ROESY peaks) is highly dependent on the correlation times for the solvent–solute interaction, and so the absence of observable effects does not indicate the absence of an interaction. Although we have observed no direct evidence for TFE binding, we note that *m*-value dependence observed in these and other peptides is consistent with TFE binding or exchange with water, can reasonably be derived from an interaction model, and has been attributed to binding in the case of urea denaturation (Pace, 1986, and references cited therein). It is certainly possible, however, that alternative considerations could account for the dependence. In particular, a similar peptide-length- and temperature-dependent *m*-value relationship between $\Delta G_{\text{helix formation}}$ and [TFE]/[H_2O] could arise from free energies of transfer of a peptide bond from water to TFE–water mixtures, as discussed for denaturants by Tanford (1968). Such a model could also account for TFE's ability to induce α-helical, rather than β-sheet, secondary structure and may be equivalent to TFE binding or exchange on a molecular level.

We have used TFE/H_2O exchange on peptide binding sites as a theoretically viable working model for analyzing the ability of TFE to promote helical structure formation in a series of peptides. Empirical observation of *m*-value dependence stands, however, and we note that equilibrium constants and *m*-values can be obtained from TFE titration curves regardless of the model chosen to explain concentration dependence. We feel that consideration of the decrease in water's activity with increasing [TFE] is important in the extrapolation of $K_{\text{helix formation}}$ from titration curves with high [TFE] midpoints. Our experiments demonstrate that additional information concerning the number of peptide residues in helix–coil equilibrium can be extracted from the *m*-value and used in conjunction with observed $[\Theta]_{222}$ values. These results indicate that TFE titration curves may produce quantitatively interpretable measurements of hidden structural propensity in peptides.

REFERENCES

Bruch, M. D., & Hoyt, D. W. (1992) *Biochim. Biophys. Acta 1159*, 81–93.

Chakrabartty, A., Schellman, J., & Baldwin, R. (1991) *Nature 351*, 586.

Conio, G., Patrone, E., & Brighetti, S. (1970) *J. Biol. Chem. 245*, 3335–3340

Creighton, T. E. (1991) *Curr. Opin. Struct. Biol. 1*, 5–16.

Doty, P., & Yang, J. T. (1956) *J. Am. Chem. Soc. 78*, 498.

Doty, P., Holtzer, A. M., Bradbury, J. H., & Blout, E. R. (1954) *J. Am. Chem. Soc. 76*, 4493.

Dyson, H. J., Rance, M., Houghten, R. A., Wright, P. E., & Lerner, R. A. (1988) *J. Mol. Biol. 201*, 201–217.

Fan, P., Bracken, C., & Baum, J. (1993) *Biochemistry 32*, 1573–1582.

Forood, B., Feliciano, E. J., & Nambiar, K. P. (1993) *Proc. Natl. Acad. Sci. U.S.A. 90*, 838.

Holtzer, M. E., & Holtzer, A. (1992) *Biopolymers 32*, 1675–1677.

Horovitz, A., Matthews, J., & Fersht, A. R. (1992) *J. Mol. Biol. 227*, 560.

Liebes, L. F., Zand, R., & Phillips, W. D. (1975) *Biochim. Biophys. Acta 405*, 27–39.

Lifson, S., & Roig, A. (1961) *J. Chem. Phys. 34*, 1963.

Lyu, P. C., Liff, M. I., Marky, L. A., & Kallenbach, N. R. (1990) *Science 250*, 669.

Nelson, J. W., & Kallenbach, N. R. (1986) *Proteins: Struct., Funct., Genet. 1*, 211–217.
Nelson, J. W., & Kallenbach, N. R. (1989) *Biochemistry 28*, 5256–5261.
O'Neil, K. T., & DeGrado, W. F. (1990) *Science 250*, 646.
Ooi, T., & Oobatake, M. (1991) *Proc. Natl. Acad. Sci. U.S.A. 88*, 2859.
Pace, C. N. (1986) *Methods Enzymol. 131*, 266.
Privalov, P. L. (1979) *Adv. Protein Chem. 33*, 167.
Richardson, J. S., & Richardson, D. C. (1988) *Science 240*, 1648.
Sancho, J., Niera, J. L., & Fersht, A. R. (1992) *J. Mol. Biol. 224*, 749.
Schellman, J. A. (1990) *Biophys. Chem. 37*, 121–140.
Scholtz, J. M., Marqusee, S., Baldwin, R. L., York, E. J., Stewart, J. M., Santoro, M., & Bolen, D. W. (1991a) *Proc. Natl. Acad. Sci. U.S.A. 88*, 2854–2858.
Scholtz, J. M., Qian, H., York, E. J., Stewart, J. M., & Baldwin, R. L. (1991b) *Bioploymers 31*, 1463–1470.
Shin, H. C., Merutka, G., Waltho, J. P., Tennant, L. L., Dyson, H. J., & Wright, P. E. (1993) *Biochemistry 32*, 6356–6364.
Sonnichsen, F. D., Van Eyk, J. E., Hodges, R. S., & Sykes, B. D. (1992) *Biochemistry 31*, 8790–8798.
Storrs, R. W., Truckses, D., & Wemmer, D. E. (1992) *Biopolymers 32*, 1695–1702.
Sueki, M., Lee, S., Powers, S. P., Denton, J. B., Konishi, Y., & Scheraga, H. A. (1984) *Macromolecules 17*, 148.
Tanford, C. H. (1968) *Adv. Protein Chem. 23*, 121.
Wojcik, J., Altmann, K. H., & Scheraga, H. A. (1990) *Biopolymers 30*, 121–134.
Zhong, L., & Johnson, W. C. (1992) *Proc. Natl. Acad. Sci. U.S.A. 89*, 4462–4465.
Zimm, B. H., & Bragg, J. R. (1958) *J. Chem. Phys. 31*, 526.